FULL PAPER

TAPE: A Medical Adhesive Inspired by a Ubiquitous Compound in Plants

Keumyeon Kim, Mikyung Shin, Mi-Young Koh, Ji Hyun Ryu, Moon Sue Lee, Seonki Hong, and Haeshin Lee**

Adhesives play an important role in industrial fields such as electronics, architectures, energy plantation, and others. However, adhesives used for medical purpose are rather under-developed compared with those used in industry and consumer products. One key property required for medical adhesives is to maintain their adhesiveness in the presence of body fluid. Here, an entirely new class of medical adhesives called TAPE is reported; this is produced by intermolecular hydrogen bonding between a well-known polyphenol compound, tannic acid, and poly(ethylene glycol). The preparation method of TAPE is extremely easy, forming a few liters at once by just the simple mixing of the two compounds without any further chemical synthetic procedures. TAPE shows a 250% increase in adhesion strength compared with fibrin glue, and the adhesion is well maintained in aqueous environments. It is demonstrated that TAPE is an effective hemostatic material and a biodegradable patch for detecting gastroesophageal reflux disease in vivo. Widespread use of TAPE is anticipated in various medical and pharmaceutical applications such as muco-adhesives, drug depots, and others, because of its scalability, adhesion, and facile preparation.

1. Introduction

Adhesives are indispensable in daily life and in industrial fields such as electronics, energy storage devices, and others, because they achieve interfacial adhesion between two different materials. However, adhesives for medical purposes are rather under-developed compared with those used in industrial and consumer products. Commercially available medical adhesives can be divided into three classes: (1) polymer-based medical glues using chitosan, gelatin, alginate, and poly(ethylene glycol) s (PEGs),[1–4] (2) cyanoacrylate derivatives,[5] and (3) fibrinogen and thrombin containing fibrin glues.[6] Each class shows advantages and disadvantages. Most of polymer-based glues are biocompatible, but some of their degradation products cause irritation on the skin or inflammatory responses on the tissues. Also, poor mechanical and adhesion properties are another problem of this class, which is mostly arising from their poor solubility in water.[7–9] Cyanoacrylate glues can strongly adhere to tissues but have limitations that arise from the inflammation caused by its toxic degradation by-products, cyanoacetate and formaldehyde.[5] Fibrin glues are more biocompatible then cyanoacrylate glue, but they weakly bind to tissues and entail a risk of infectious transmission from the human blood plasma donor.[6] Recently, aldehyde-based tissue adhesives have been developed.[10,11] These adhesives exhibited fairly good tissue adhesion with suitable biocompatibility, but chemical conjugation is always necessary, which often results in batch-to-batch variations. Thus, the issues to address include body-fluid-resistant adhesion, scalability, and material safety.

Tannins are polyphenol compounds that are found ubiquitously in virtually all plant species. They have drawn significant attention for their multifunctionalities, including their antioxidant, anti-mutagenic, anti-carcinogenic, and anti-bacterial properties.[12–14] Tannic acid (TA) (chemical structure shown in **Figure 1**A) is a representative hydrolysable tannin. In addition to the aforementioned properties, TA has shown intermolecular interactions with polymers such as PEG, poly(N-isopropylacrylamide) (PNIPAM), and poly(N-vinylpyrrolidone) (PVPON).[15–18] TA acts as a molecular glue, forming three-dimensional intermolecular networks and resulting in the stable formation of layer-by-layer (LbL) thin films.[19–21] Furthermore, TA-mediated polymeric microcapsules and micelles exhibiting pH-responsive degradable properties for drug delivery and live cell encapsulation have been reported.[22–25]

Here, we report a chemically defined, readily scalable medical adhesive called TAPE, inspired by the adhesive properties of a well-known degradable polyphenol, TA. We found that preparation of a simple mixture of TA (1 g mL^{-1} in distilled water) and PEG (1 g mL^{-1} in distilled water) resulted in wet-resistant adhesives that showed high adhesion strength (up to ≈kPa) compared to fibrin glues, with an approximately 250%

K. Kim, M. Shin, Dr. J. H. Ryu, Prof. H. Lee
The Graduate School of Science and Technology, KAIST
291 Daehak-ro, Yuseong-gu, Daejeon 305-701
South Korea
E-mail: haeshin@kaist.ac.kr
K. Kim, Dr. M.-Y. Koh, Dr. M. S. Lee
InnoTherapy Inc.
97 Uisadang-daero, Yeongdeungpo-gu, Seoul 150-737, South Korea
Dr. S. Hong, Prof. H. Lee
Department of Chemistry, KAIST
291 Daehak-ro, Yuseong-gu, Daejeon 305-701, South Korea
E-mail: ywan00@kaist.ac.kr

DOI: 10.1002/adfm.201500034

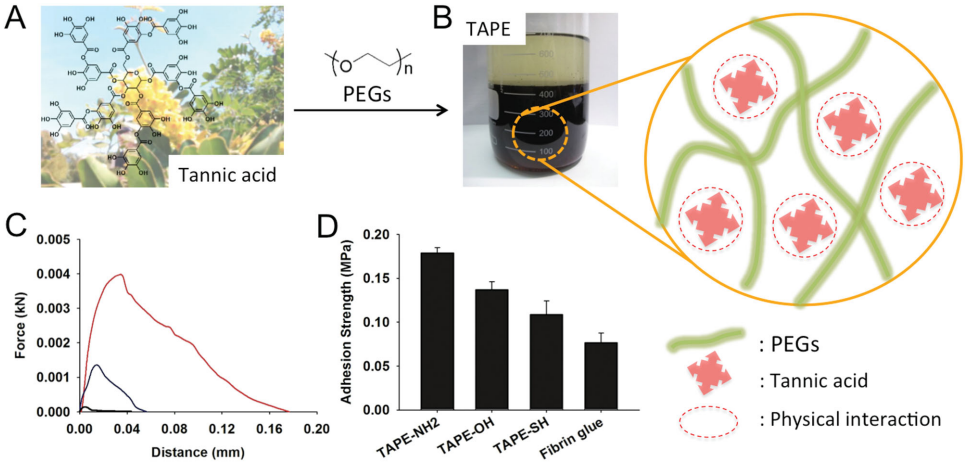

Figure 1. Formation of TAPE. A) Tannic acid (TA), one of the major components in hydrolysable tannins found in secondary metabolites of plants. B) Mass-produce TAPE at the laboratory scale (500 mL of TAPE) by mixing TA with PEG. C) Force–distance curves of TAPE–NH_2 (red) compared to TA (blue) and PEG–NH_2 (black). D) Adhesion strength of TAPE with different terminal functional groups of PEG (–NH_2, –OH, and –SH) and fibrin glue as a positive control.

increase. Because synthetic procedures are not involved, a few liters of TAPE can be readily prepared at once. The end functional groups of the PEG affects the adhesion strength of TAPE (R-NH_2 > R-SH > R-OH), as does the number of PEG arms. Our results revealed that virtually all hydroxyl groups of TA and the ethylene glycol units of PEG were interconnected to form robust molecular networks, exhibiting superior adhesion. TAPE acts as an effective hemostatic material and a pH-sensing adhesive probe for the diagnosis of gastroesophageal reflux disease (GERD), suggesting that as a new adhesive platform, TAPE can be widely used for many biomedical applications.

2. Results and Discussion

The method to prepare TAPE is extremely easy. First, TA (1 g of TA dissolved in 1 mL of distilled water) and PEG (1 g of PEG dissolved in 1 mL of distilled water) solutions were separately prepared. Second, the two solutions were mixed with different volume ratios (typically 2:1). When mixing the two solutions, a highly viscous water-immiscible liquid settled down immediately, as shown in Figure 1B. Because no chemical synthetic procedure is involved, a large volume of TAPE can be prepared with ease. For example, more than 500 mL of TAPE could be made at the laboratory scale at once (Figure 1B).

The adhesion strength of TAPE is surprisingly higher than that of each individual component. The adhesion strengths of TA, PEG, and TAPE were measured by a universal testing machine (UTM). TA, PEG, or TAPE was applied on the epidermic side of porcine skin (a bottom tissue, diameter: 6 mm), then, it was covered with another piece of skin as depicted in Figure S1, Supporting Information. Detachment force values were low for each component: 0.0002 kN for PEG (Figure 1C, black) and 0.001 kN for TA (blue). However, the detachment force for the mixture of the two components, TAPE, increased fourfold to 0.004 kN (red). Note that the detachment force of TAPE did not rapidly decrease after the maximum point but instead showed a gradual decrease to the distance approximately 16 mm. This result indicates the extensive degrees of intermolecular interactions between TA and PEG in TAPE solution. The adhesion strength of TAPE, defined as an adhesion force divided by a contact area, varied depending on the end-functional groups of the PEG. We selected 10 kDa branched PEG with four arm configurations. The only differences are the end-group moieties with amine-(PEG–NH_2), hydroxyl-(PEG–OH), and thiol-(PEG–SH) terminations. TAPE using PEG–NH_2, designated by TAPE–NH_2 showed the highest adhesion strength (≈0.18 MPa), followed by TAPE–OH and TAPE–SH. Although TAPE showed changes in adhesion strength depending on the mixed PEG, all TAPEs revealed higher adhesion strengths than that of the commercially available medical adhesive, fibrin glue (≈0.07 MPa) (Figure 1D). Overall, the TAPE–NH_2 exhibited a 250% increase in adhesion strength over fibrin glue.

We investigated the mechanism of TAPE formation. We used TAPE–NH_2 as a model system because it showed the highest adhesion force. First, gel-permeation chromatography (GPC) was performed to prove the intermolecular interactions between TAs and PEGs. Because PEG itself is not UV-responsive at the wavelength of 280 nm, we can easily separate TA-bound PEG species detected by UV-based sensor at 280 nm after separating from GPC column. The 10 kDa PEG–NH_2 was eluted at a retention time of 17.7 min in the GPC setting confirmed by a refractive index detector (Figure S2A, Supporting Information). Because it is not UV-responsive, there was no peak detected by the UV-based sensor (black line, **Figure 2**A). When adding TA with PEG, it showed three major peaks; one was eluted at 17.2 min corresponding to the TA-bound PEG with increased hydrodynamic volume, another was eluted at 19 min which might be the aggregated complex of TA/PEG with collapsed volume compared with PEG itself, and last one was unbound TA shown at 29.8 min. The retention time of unbound TA was double-checked with the peak of TA injected alone shown in Figure S2B, Supporting Information. We interpreted that two peaks of TA/PEG complexes showed strong interaction between TA and PEG under the influence of the ionic strength of the phosphate-buffered saline (10×10^{-3} M, pH

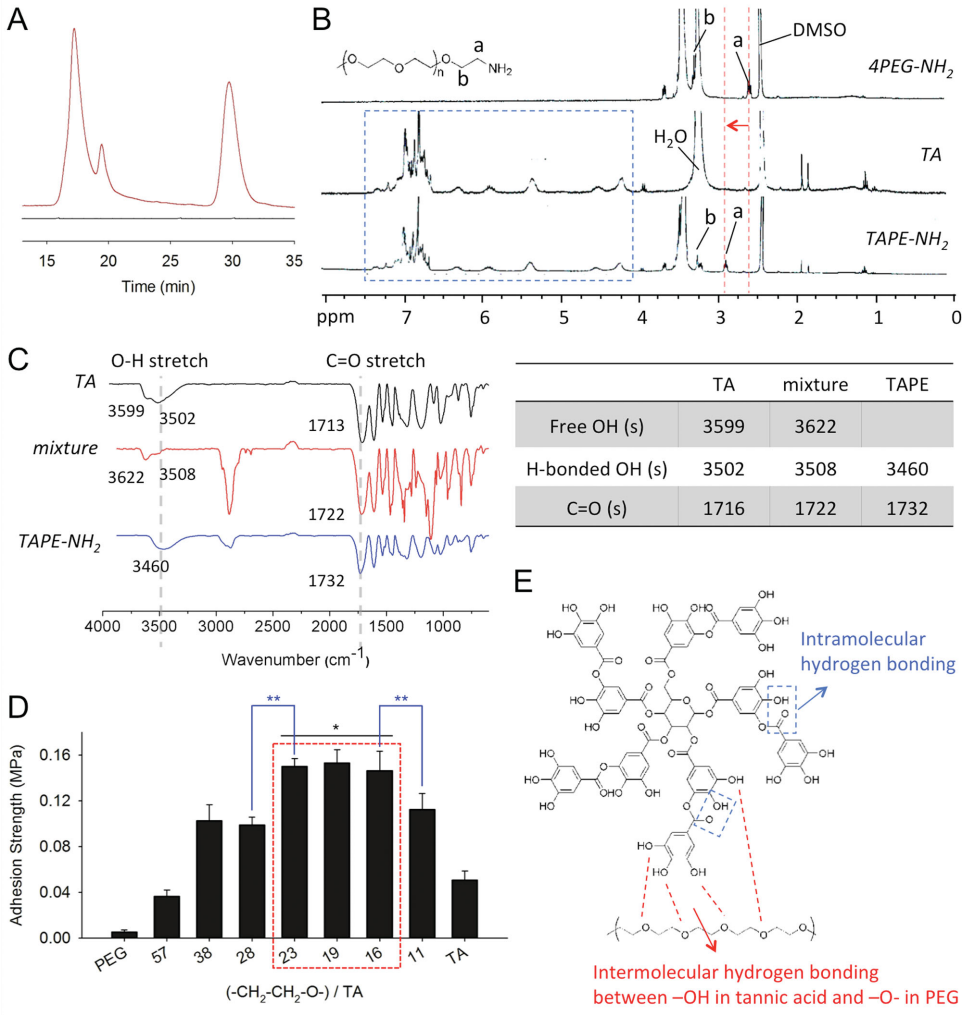

	TA	mixture	TAPE
Free OH (s)	3599	3622	
H-bonded OH (s)	3502	3508	3460
C=O (s)	1716	1722	1732

Figure 2. Intermolecular hydrogen bonding confirmation by various analytical tools. A) GPC data of PEG (black) and PEG after contact with TA at a sufficiently low concentration to be water-soluble (red) detected by UV-based sensor. B) ^{1}H-NMR data of TAPE and its starting materials, TA and 4-arm-PEG–NH_2. C) Chemical shift analysis of the hydroxyl group (O–H) and carbonyl group (C=O) in TA by FT-IR spectroscopy. D) Adhesion strength of various TAPEs with different ethylene glycol/TA molecular ratios (n = 5). * indicates statistical significance of $p > 0.05$ with one-way ANOVA test. ** indicates statistical significance of $p < 0.05$ with t-test. E) Hypothetical molecular interaction between TA and PEG.

4.0, eluent). Second, nuclear magnetic resonance (NMR) spectroscopy was used. We dissolved TAPE in a variety of organic solvents to find the way of disassembling TAPE to investigate the driving force forming TAPE. The TAPE-NH_2 was only dissolved in dimethyl sulfoxide (DMSO), not in acetone, ethanol, methanol, hexane, and toluene (Figure S3, Supporting Information), saying the formation of TAPE was much related to hydrogen bonding interaction because DMSO is a well-known solvent to interfere the preformed hydrogen bonding by intercalation. So, NMR analysis was performed using DMSO-d_6 as a solvent to describe further chemical environments changed by TAPE formation followed by disassembly. We compared the ^{1}H-NMR peaks of TAPE dissolved in DMSO-d_6 with those of TA and PEG dissolved in DMSO-d_6 separately. The blue-dotted box in Figure 2B shows exactly the same NMR peaks between TA and TAPE, indicating that there are no changes in the chemical environment of the TA that later forms TAPE. For PEG, however, one change was observed. A peak appeared at 2.6 ppm for PEG-NH_2, which was assigned to the –CH_2– located next to terminal primary amine group (a, in the upper spectrum of Figure 2B). This proton peak was shifted downfield to 2.9 ppm, suggesting that the change might be caused by the protonation of the amine group when PEG was mixed to TA to form TAPE, due to the low pH of the aqueous solution of TA (TA solution: pH ≈ 2.6, PEG solution: pH ≈ 9.4, and the supernatant after TAPE formation: pH ≈ 2.6). The change in chemical shift of CH_2 next to the amine in TAPE was exactly the same as that in PEG-NH_2 alone in DMSO-d_6 with slight amount of DCl to drop the pH (Figure S4, Supporting Information). However, the environmental changes occurred in the H from the amine group of PEG could not be directly detected by ^{1}H-NMR because of the fast H-D exchange. The aforementioned ^{1}H-NMR data also suggest that no covalent bonds were newly formed. Third, we performed Fourier Transform Infrared (FT-IR) spectroscopy measurement. In the FT-IR spectrum, a wavenumber shift related to the hydroxyl groups (–OH) and the carbonyl groups (C=O) in TA

was observed (Figure 2C). Before TAPE formulation, two species of hydroxyl groups were found in TA, free/unbound –OH (3599 cm^{-1}) and hydrogen bonded (H-bond) hydroxyl groups (3502 cm^{-1}) (upper line in Figure 2C). However, the two species became one because nearly all hydroxyl groups participated in H-bonding after TAPE formulation (bottom line in Figure 2C). The hydroxyl group (3502 cm^{-1}) participating in the H-bond shifted to 3460 cm^{-1} after TAPE formulation, indicating the weakened vibrational energy of the O–H bonding, which might be caused by interactions with the ether group (–O–) of PEG in TAPE. As a control experiment, the PEG and TA powders were physically mixed, and a FT-IR spectrum was obtained. A negligible peak shift for the –OH and C=O chemical groups in TA was observed, indicating little H-bonding interactions in the powder phase (Figure 2C, middle line). Furthermore, the C=O vibration in TA was increased from 1713 cm^{-1} (free TA) to 1739 cm^{-1} (TA in TAPE), indicating that the strengthened vibrational energy of the C=O bonding was affected by interacting with the hydrogen donor, –OH. These two chemical energy shift shown in FT-IR were exactly corresponding to the previous study,[26] clearly supporting that the –OH and C=O in TA both participate in forming the hydrogen bonds that are responsible for the unique characteristics observed in TAPE. TAPE was only formed at acidic pH (Figure S5, Supporting Information) because the hydrogen bonding, which is its major driving force, was not occurred in basic pH due to the deprotonation. In neutral pH, gum-like aggregate was formed and settled down, but this had not showed any adhesive force at all. There was no aggregate formed in basic pH (Figure S5, Supporting Information).

A stoichiometric study was performed by changing the molar ratios of TA and PEG, which can be useful quantitative information concerning the aforementioned H-bond character. The adhesion strength of TAPE made by TA with various molar ratios of PEG is shown in Figure 2D. The molar ratio of TA and PEG was calculated by the number of ethylene glycol (EG) groups interacting with one TA molecule (i.e., # of $–CH_2–CH_2–O–$ per TA). The adhesion strength was increased as the ratio of EG was increased up to 19 units to one TA molecule and then gradually decreased upon further increases in the ratio of EG to 57. The 16 to 23 EG units showed the strongest adhesion strength in Figure 2D (red-dotted box). These data might reflect that the EG to TA ratio of 16 to 23 exhibiting the strongest adhesion indicates an optimal molecular interaction between EGs and TA with the fewest unbound functional groups. The 16 to 23 units of –O– in EGs are acceptors bonded with the 16 to 23 units of –OH in one TA molecule. The total number of –OH in TA is 25 units, as shown in Figure 2E. Thus, residual 2 to 9 units of –OHs in TA can participate in intramolecular hydrogen bonding with the five C=O groups in TA (Figure 2E, blue-dotted box). In fact, our interpretation is confirmed by the previous FT-IR data showing the chemical shift of C=O in TA after forming TAPE, thus indicating physical interaction participation (Figure 2C). From our spectroscopic results and simple numeric calculations, we tentatively conclude that most –OH units in TA intermolecularly interact with –O– in PEG and some –OH units in TA intramolecularly interact with C=O groups in TA by hydrogen bonding, as described in Figure 2E (red-dotted line).

One unique property of TAPE adhesion is its reversibility, similar to the adhesion shown in the commercial Post-It. We measured the adhesions of TAPE–NH_2 and TAPE–OH. During the first attachment and detachment experiment by UTM, the adhesion strength of TAPE–NH_2 (≈0.2 MPa) was greater than that of TAPE–OH (≈0.1 MPa) (**Figure 3**A). Later in time, the adhesion strengths of both TAPEs were gradually increased until 30 cycles of attachment and detachment (≈0.26 MPa for TAPE–NH_2 and ≈0.17 MPa for TAPE–OH). For TAPE–NH_2, the adhesion force was gradually decreased down to 0.05 MPa after 100 cycles (Figure 3A, red). A different tendency was

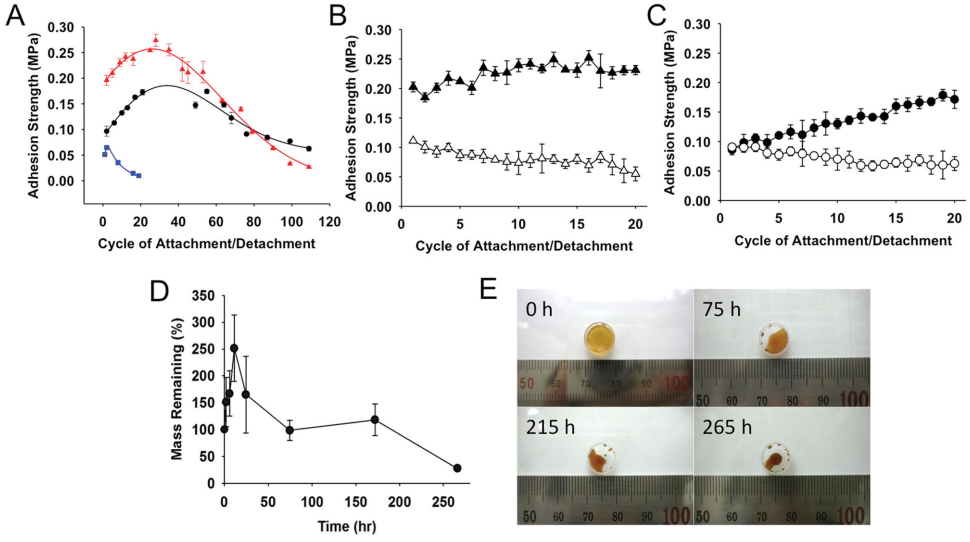

Figure 3. Characterization of the adhesion strength of TAPE. A) The adhesion strength of TAPE–NH_2 (red) and TAPE–OH (black) compared to that of TA (blue), depending on the number of repeated attachment/detachment processes ($n = 3$). B) The adhesion strength of TAPE–NH_2 in the absence (unfilled) and presence of water (filled) ($n = 3$). C) The adhesion strength of TAPE–OH in the absence (unfilled) and presence of water (filled) ($n = 3$). D) In vitro degradation test of TAPE–OH in PBS (1×, pH 7.4, and 37 °C). E) Photographic images of the TAPE–OH at each time of degradation test.

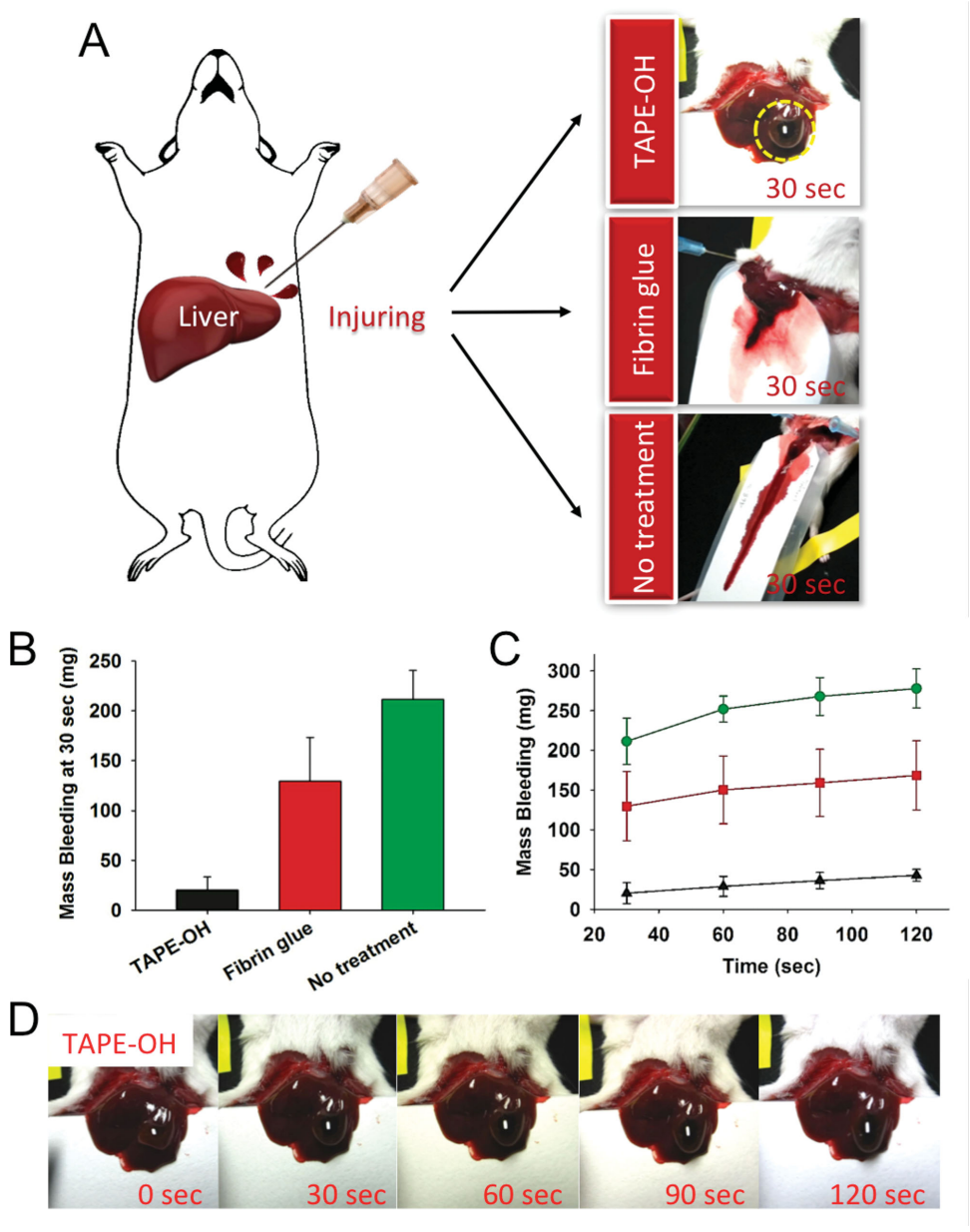

Figure 4. Hemostatic ability of TAPE–OH. A) A schematic illustration of the mouse liver hemorrhage model and photographs of the bleeding level of the damaged liver treated by TAPE–OH or fibrin glue (positive control), and untreated (negative control) at 30 s after the injury. B) The amount of bleeding at 30 s after the injury (black: TAPE–OH, red: fibrin glue, and green: no treatment). Significance was tested by one-way ANOVA test ($p < 0.05$). C) The accumulated amount of bleeding every 30 s until stopped (2 min) ($p < 0.05$, with one-way ANOVA test). D) Snapshots of a TAPE–OH treated liver every 30 s for 2 min.

observed for TAPE–OH, in which the adhesion force was well maintained up to approximately 60 cycles and then decreased to ≈0.1 MPa (black). From the results, it was demonstrated that the adhesion strength and its sustainability could be modulated by changing the type of PEG mixed. TAPE–OH exhibited better sustainability in adhesion, but TAPE–NH_2 showed stronger adhesion. Interestingly, the reversible adhesive property of TAPEs was relatively well maintained in the presence of water, although the initial adhesion force was decreased from ≈0.2 to ≈0.1 MPa for TAPE–NH_2 (Figure 3B) and ≈0.1 MPa for TAPE–OH (Figure 3C). The adhesion strengths of both TAPEs were well maintained for 20 cycles of attachment and detachment in water (Figure 3B,C, unfilled). The level of wet adhesion (≈0.1 MPa) was suitable for various in vivo experiments shown later (**Figures 4** and **5**). In vitro degradation of TAPE was investigated by gravimetric analysis, as shown in Figure 3D. TAPE–OH was incubated in phosphate buffered saline (PBS) solution (pH 7.4) at 37 °C with gentle stirring. The PBS was completely removed, and the weight of remaining glue was measured at predetermined time intervals. The weight of TAPE–OH rapidly increased due to the absorbance of water within the first few hours and then decreased. After 11 d, approximately 80%

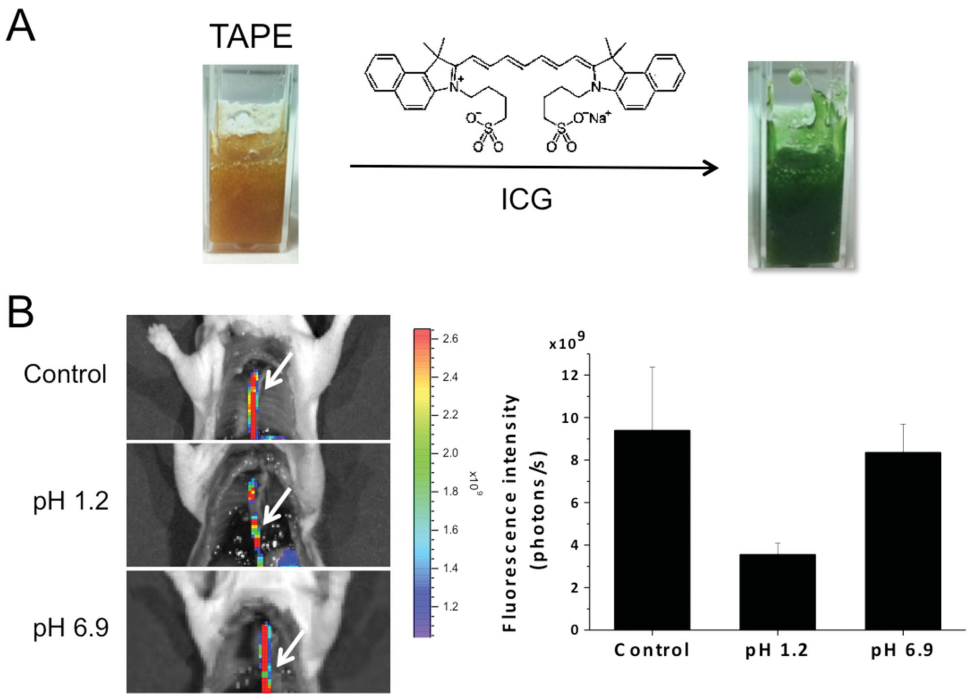

Figure 5. ICG-encapsulated TAPE as a bioadhesive pH-sensing probe. A) Formation of ICG-encapsulated TAPE. B) In vivo fluorescence intensity of the ICG-encapsulated TAPE in esophagus. Control: ICG-encapsulated TAPE without any solution (up). pH 1.2: ICG-encapsulated after exposure to artificial gastric juice for 10 min (middle). pH 6.9: ICG-encapsulated after exposure to artificial intestinal liquid for 10 min (bottom).

of the initial weight of TAPE–OH disappeared (Figure 3D). Photographic images of the in vitro degradation of TAPE–OH are shown in Figure 3E. Degradation profile of TAPE was also dependent to the end functional group of PEG at different pH. In this experiment, we monitored the release profile of pyrogallol from the TAPE immersed in the PBS at pH 2 and 10. Pyrogallol is a representative degradation product of TAPE. For TAPE–OH, pyrogallol was almost released out regardless of the pH of surrounding (Figure S6A, Supporting Information). However in the case of TAPE–NH_2 immersed in pH 10, only 70% of pyrogallol was recollected from TAPE (Figure S6B, Supporting Information) because of the oxidation reaction of TA at basic pH followed by covalent bond-forming reaction with the amine group in PEG. In pH 2, TAPE–NH_2 also completely degraded, saying there were no newly formed covalent bonds in acidic pH the same as its early state of formation.

The hemostatic ability of TAPE–OH was investigated by using a mouse liver bleeding model. Bleeding was initiated by pricking a liver with an 18-gauge needle, and we measured the amount of blood from each group. The first group was a negative control, meaning that no attempt for hemostasis was made. The second group was fibrin-treated mice (positive controls), and the third group was the application of TAPE–OH (Figure 4A). The photographic images show snapshots of the bleeding sites of each group after 30 s. The two groups treated by the hemostatic agents of fibrin or TAPE–OH showed reductions in the bleeding amount. The amount of bleeding measured for the first 30 s timeframe (i.e., 0–30 s) was 20.2 mg (±13.09 mg) for TAPE–OH treated group, 129.6 mg (±43.58 mg) for the fibrin-treated, and 211.2 mg (±29.15 mg) for the negative control (Figure 4B). The significant difference was found between TAPE–OH and control groups with one-way ANOVA test ($p < 0.05$). We monitored subsequent bleeding with an interval of 30 to 120 s. As shown in Figure 4C, the accumulated amounts of bleeding were all saturated after 120 s, indicating completed hemostasis. However, the total amount of blood measured exhibited significant differences ($p < 0.05$, with one-way ANOVA test). The total amount at 120 s was 42.7 mg (±7.51 mg) for the TAPE–OH treated group, 168.5 mg (±43.62 mg) for the fibrin glue treated, and 277.7 mg (±24.51 mg) for the negative control (Figure 4C). The actual photographs of the hemostatic effect of TAPE–OH on liver bleeding at each sampling period in Figure 4C are presented in Figure 4D. The TAPE–OH stopped bleeding efficiently by adhering and covering the injury site completely even though blood from the initial bleeding was present at the liver tissue. These snapshots demonstrated that the mass bleeding of TAPE–OH was significantly reduced compared with the control groups. Thus, we demonstrated that TAPE has a significant potential as a local hemostatic agent.

In addition, we demonstrated the ability of TAPE–OH for detecting GERD because of its maintenance of wet-adhesive properties. In GERD, gastroesophageal reflux rapidly decreases the pH values to between 1 and 2, which damages the tissue surfaces of the esophagus. Diagnosis of GERD is based on monitoring the sudden pH drop caused by the reflux of stomach acid to the esophagus. Inserting a pH probe to the esophagus of potential GERD patients through an oral track and maintaining it for several hours or even a day is a painful process. We hypothesized that use of TAPE encapsulating fluorescent molecules could be a patient-friendly approach to the diagnosis of GERD. At low pH, the five ester bonds in TA result in rapid degradation of TAPE,[27] thus releasing the encapsulated

fluorescent molecules, which leads to the diagnosis of GERD. The decrease in fluorescent signals resulting from the reflux of stomach acid is expected to be observed in GERD animal models. For this purpose, we prepare indocyanine green (ICG) encapsulated TAPE (ICG-TAPE–OH). ICG is a clinical imaging agent approved by the Federal Drug Administration (FDA) for human use, and the electrons in ICG are excited by near infrared, radiating fluorescent light during relaxation of electrons to ground states (Figure 5A).[28] The in vivo pH-sensing ability of the ICG-TAPE–OH was investigated in the mouse esophagus. The animal model for the detection of GERD was prepared through introduction of TAPE in the esophagus by an oral injection followed by monitoring the fluorescence during feeding of artificial gastric juice (pH 1.2) (experimental details are available in Experimental Section). In Figure 5B, the fluorescence intensity measured after TAPE–OH introduction was 9.4 ± 2.97 ($\times 10^9$) (control). The intensity measured after oral injections of artificial intestinal liquid with a pH value of 6.9 was 8.4 ± 1.33 ($\times 10^9$), similar to the initial intensity. However, the artificial gastric juice (pH 1.2) significantly reduced the fluorescence intensity of ICG-TAPE–OH even in 10 min (3.6 ± 0.52 ($\times 10^9$)). The experimental timeframe of 10 min was determined from the previous report in which the hydrolysable tannin is degraded rapidly within 10 min. The in vivo result indicates that the ICG-TAPE–OH can be a useful pH sensor for diagnosing GERD due to the adhesive and encapsulating properties of TAPE, potentially being an alternative method that can be used in clinical settings. In fact, poly(ethylene) glycol, tannic acid, and ICG are compounds that have already been approved for human use.

3. Conclusion

We developed an entirely new class of medical adhesives called TAPE that is inspired by a ubiquitous compound in plants, tannic acid. TAPE was spontaneously prepared on a large scale by strong intermolecular hydrogen bonding between the hydroxyl group in TA and the ether group in PEG. This scalability was originated by the simple mixing processes of PEG and TA. In fact, TAPE can be prepared on a liter scale in a day, even on a small laboratory scale. TAPE showed 250% increases in adhesive strength compared to the widely used fibrin glue, and the adhesion was very effective, even in the presence of water. TAPE showed good hemostatic ability. Furthermore, TAPE with encapsulated ICG could be applied as an adhesive pH-sensitive probe for the detection of gastroesophageal reflux disease. We expect that its application to a variety of medical and pharmaceutical purposes such as mucoadhesives and drug depots will open new avenues of TAPE studies.

4. Experimental Section

TAPE Formation: TAPE was immediately formed and settled down after mixing 671 µL of TA (Sigma-Aldrich, St. Louis, MO, USA) solution in distilled water (50% w/w) with 329 µL of PEG (4-arms, 10 kDa) solution in distilled water at the same concentration. After mixing, the mixed TA and PEG solution was centrifuged for 3 min at 13 500 rpm to collect TAPE, and then the supernatant was removed. We used PEG with different molecular weights (4.6 kDa, 10 kDa), branching (2, 4-arms), and end-functional groups including –NH_2, –OH, and –SH. (PEG–NH_2, PEG–OH, and PEG–SH, 10 kDa), all of which were purchased from SunBio, Inc. (Korea) and Sigma-Aldrich.

^{1}H-NMR Analysis of TAPE: To understanding the covalent bonding integration in forming TAPE, we performed ^{1}H-NMR analysis of TAPE (using PEG–NH_2, 10 kDa) after dissolving in DMSO-d_6 (Sigma-Aldrich, St. Louis, MO, USA). We compared the chemical shift of TAPE in DMSO-d_6 with that of TA and PEG in DMSO-d_6 separately by using a Bruker AVANCE 400 spectrometer. ^{1}H-NMR (400 MHz, DMSO-d_6, δ) of TAPE: 7.19 (s, 1H, $C_6H_2H(OH)_2$–), 6.81-6.88 (m, 2H, C_6HH_2–$(OH)_2$–), 4.09-4.05 (m, 2H, –NH–CH_2–$C_6H_3(OH)_2$–), 3.95-3.59 (m, PEO), 3.40-3.36 (t, 2H, PEO–CH_2–NH–).

GPC Analysis: The molecular interaction of TA and PEG was determined by gel permeation chromatography (GPC). Two GPC columns (OHpak SB-806M HQ and SB-804 HQ, Shodex, Munich, Germany) were connected in series and equilibrated with phosphate-buffered saline (10×10^{-3} M, pH 4.0, eluent). The flow of eluent was 1 mL min^{-1}, and the injection volume was 10 µL. The columns were first characterized with the starting materials; TA (Elution time: 19.5 min) and PEG (PEG–NH_2, star shaped, 10 kDa, Elution time: 17.5 min). 70 µL of TA solution (10 mg mL^{-1} in distilled water) was mixed with 980 µL of PEG solution (10 mg mL^{-1} in distilled water, PEG–NH_2, 10 kDa). The mixed solution was filtered with a 0.2 µm pore-sized syringe filter and then analyzed by GPC each hour for 10 h. The materials separated by the GPC column were detected by UV–vis spectrometry at a wavelength of 280 nm.

FT-IR Analysis: The Fourier transform infrared (FT-IR) spectrum was obtained using a Bruker Equinox-55 FT-IR spectrophotometer using a KBr pellet. We measured the FT-IR spectrum of TAPE (PEG–NH_2, 10 kDa) after lyophilizing and compared this spectrum with that of a mixture with TA and PEG in their powder forms without any interaction in a solution phase.

Adhesion Strength of TAPE with Various Molar Ratio of EG Monomers to TA: First, TAPEs with various molar ratios of EG to TA were prepared by a method described above. Adhesion testing of TAPE was performed by a universal testing machine (UTM, INSTRON 5583, Figure S1, Supporting Information) using porcine skin tissue. A biopsy punch (Miltex REF 33-36) was used to cut porcine skin tissue with a diameter of 6 mm. Then, the porcine skin tissues were attached to two rods of a system designed to determine adhesion strength using an instant adhesive (Aron alpha, Toagosei Co., LTD, Japan), as shown in Figure S1, Supporting Information. The TAPE was applied uniformly between two layers of pig skin tissues in an amount of approximately 3 mg. The porcine skin tissues with TAPE were attached and detached continuously ten times by the experimenter's hands, and then two rods were installed in the UTM (Figure S1, Supporting Information). A UTM test was performed to apply a force of 20 N to the samples for 1 min, and after that a tensile force was applied thereto at a rate of 1 mm min^{-1} to determine the adhesion strength. Each sample of TAPE with a different molar ratio of PEG was tested five times continuously, and the average adhesion strength was measured.

Force–Distance Curve: TA solution, PEG–NH_2 solution at a concentration of 50% (w/w) in distilled water and TAPE–NH_2 (molar ratio, EGs:TA = 16:1) were prepared to determine the force–distance (F–D) curve. The method used to measure the F–D curve was same as the adhesion strength test.

Adhesion Strength of TAPE with Different Terminal Functional Groups: TAPE–NH_2, TAPE–OH, and TAPE–SH with an EG to TA molar ratio of 16 were prepared. Fibrin glue (Beriplast P combi-set, CSL Behring, Germany) was used as a positive control to compare the adhesion strength of TAPEs. The adhesion strength of TAPE with different terminal functional groups was determined in the same manner as described above.

Monitoring of Variation in Adhesion Strength and Maintenance Time Depending on Number of Repeated Adhesion Tests: TAPE–NH_2, TAPE–OH, and TA solution (50% w/w) were prepared in the same manner as described above. To determine the adhesion strength of TAPEs and TA,

the same method for adhesion strength testing was performed over a hundred times for a few hours. Adhesion strength tests were repeated to determine variations in adhesion strength depending on the number of repeated adhesion tests. All experimental groups were tested in triplicate.

Water Resistance of TAPE: TAPE–NH_2 and TAPE–OH were prepared to investigate the water resistance of TAPE. In the same manner as described in the adhesion strength test section, TAPEs were applied uniformly on porcine skin tissues having a diameter of 6 mm in an amount of approximately 3 mg. Then, 20 μL of distilled water was applied between samples. UTM was used to apply a force of 20 N to the samples for 1 min, and then a tensile force was applied thereto at a rate of 1 mm min^{-1} to determine the water resistance adhesion strength of TAPE. The second test to the 20th test were carried out by applying 20 μL of distilled water to the samples each time and then applying a force of 20 N to the samples for 1 min and applying a tensile force thereto at a rate of 1 mm min^{-1} under the same condition as in the first test. All experimental groups were tested in triplicate.

Hemostatic Ability of TAPE: To evaluate the in vivo hemostatic ability of TAPE, we used a mouse hemorrhaging liver model.[29] Fifteen ICR mice (normal ICR mouse, 30–35 g, 6 weeks, male) were anesthetized by an intraperitoneal injection of tiletamine-zolazepam (Zoletil, Virbac) and xylazine (Rompun, Bayer). For statistical analysis, we used five ICR mice for each experimental group ($n = 5$). Bleeding on the liver was induced using an 18G needle, and 100 μL of TAPE (4.6 kDa, molar ratio of EGs:TA = 15:1) or fibrin glue (Beriplast P combi-set, CSL Behring, Germany) was immediately applied on the surface of bleeding site. At every 30 s interval, the mass of bleeding was obtained for 2 min. No treatment after the liver was pricked with a needle was considered as a negative control. Fibrin glue was used as a hemostatic agent for a positive control. Additionally, the mass of the excess fibrin glue that oozed out during the hemostat formation at first 30 s interval was examined three times, and the average was subtracted. The authors followed the ethical protocol provided by the Korean Ministry of Health and Welfare.

In Vitro Degradation Behavior of TAPE: The degradation behavior experiments of TAPE–OH (molar ratio of EG to TA = 15:1) were determined by gravimetric analysis. An EP tube cap (1.5 mL) was cut and attached to a Petri dish (90 × 15 mm) using an instant adhesive (Aron alpha, Toagosei CO., LTD, Japan). The prepared Petri dish with an EP tube cap was weighed (W_C) and then filled with 50 mg of TAPE–OH. The initial weight (W_0) of TAPE–OH and the Petri dish with an EP tube cap was defined as "W_C + 50 mg of TAPE–OH." TAPE–OH was immersed in 35 mL of the PBS buffer solution (1×, pH 7.4). During incubation, the samples were slightly shaken by an orbital shaking incubator at 50 rpm and 37 °C. At predetermined time intervals, the PBS buffer solution was removed completely using nitrogen gas blowing, and the Petri dish with TAPE–OH was weighed (W_t). After the weighing, the buffer solution was refreshed. The relative remaining weight (%) was as the following equation. All samples were in quintuplicate.

$$\text{Relative remaining weight}(\%) = (W_t - W_c)/(W_0 - W_c) \times 100$$

Synthesis of the ICG-Encapsulated TAPE–OH: ICG was obtained from Sigma-Aldrich (St. Louis, MO, USA). To synthesize the ICG-encapsulated TAPE–OH, 50% (w/w) TA solution, and 50% (w/w) PEG–OH solution were prepared in deionized water. 945 μL TA solution, 555 μL PEG solution, and 7 mg ICG were mixed vigorously. Afterwards, the resultant was centrifuged at 3000 rpm for 5 min and the supernatant solution was removed. The remainder was incubated at 60 °C for 5 min to eliminate the remaining water drops.

In Vivo pH-Sensing Ability of the ICG-Encapsulated TAPE–OH: To investigate the in vivo pH-sensing ability of the ICG-encapsulated TAPE–OH for the modeling of the GERD detection, three groups of nude mice (BALBc nude mouse, 8 weeks, male, $n = 3$) were prepared. First, each mouse was fed on 0.02 cc of the ICG-encapsulated TAPE–OH for the adhesion to the esophagus without any anesthesia. The control group was not fed any solution, but the sample groups were fed artificial gastric juice (pH 1.2) or artificial intestinal liquid (pH 6.9) for 10 min. The mice were sacrificed after 15 min, and liver, lung, and heart were dissected for the fluorescence imaging of the esophagus. The fluorescence intensity of the esophagus was measured by an IVIS 200 imaging system (Xenogen, CA, USA).

Supporting Information

Supporting Information is available from the Wiley Online Library or from the author.

Acknowledgements

This study was supported by National Research Foundation of South Korea: Mid-career scientist grant (2014002855), and Ministry of Industry, Trade, and Natural Resources: World Premier Material Development Program. This work is also supported by in part by Center for Nature-inspired Technology (CNiT) in KAIST Institute for NanoCentury (KINC).

Received: January 4, 2015
Revised: February 19, 2015
Published online: March 16, 2015

[1] R. Jayakumar, M. Prabaharan, P. T. Sudheesh Kumar, S. V. Nair, H. Tamura, *Biotechnol. Adv.* **2011**, *29*, 322.
[2] M. K. McDermott, T. Chen, C. M. Williams, K. M. Markley, G. F. Payne, *Biomacromolecules* **2004**, *5*, 1270.
[3] R. Bitton, E. Josef, I. Shimshelashvili, K. Shapira, D. Seliktar, H. Bianco-Peled, *Acta Biomater.* **2009**, *5*, 1582.
[4] C. E. Brubaker, H. Kissler, L.-J. Wang, D. B. Kaufman, P. B. Messersmith, *Biomaterials* **2010**, *31*, 420.
[5] P. A. Leggat, D. R. Smith, U. Kedjarune, *ANZ J. Surg.* **2007**, *77*, 209.
[6] T. E. MacGillivray, *J. Card. Surg.* **2003**, *18*, 480.
[7] A. P. Duarte, J. F. Coelho, J. C. Bordado, M. T. Cidade, M. H. Gil, *Prog. Polym. Sci.* **2012**, *37*, 1031.
[8] Y. C. Choi, J. S. Choi, Y. J. Jung, Y. W. Cho, *J. Mater. Chem. B* **2014**, *2*, 201.
[9] C. Ghobril, M. W. Grinstaff, *Chem. Soc. Rev.* **2015**, DOI: 10.1039/C4CS00332B.
[10] N. Artzi, T. Shazly, A. B. Baker, A. Bon, E. R. Edelman, *Adv. Mater.* **2009**, *21*, 3399.
[11] D.-A. Wang, S. Varghese, B. Sharma, I. Strehin, S. Fermanian, J. Gorham, D. H. Fairbrother, B. Cascio, J. H. Elisseeff, *Nat. Mater.* **2007**, *6*, 385.
[12] N. S. Khan, A. Ahmad, S. M. Hadi, *Chem. Biol. Interact.* **2000**, *125*, 177.
[13] K. M. Riedl, A. E. Hagerman, *J. Agric. Food. Chem.* **2001**, *49*, 4917.
[14] T. G. Shutava, S. S. Balkundi, P. Vangala, J. J. Steffan, R. L. Bigelow, J. A. Cardelli, D. P. O'Neal, Y. M. Lvov, *ACS Nano* **2009**, *3*, 1877.
[15] K. C. Yen, E. M. Woo, *Polym. Bull.* **2009**, *62*, 225.
[16] E. Costa, M. Coelho, L. M. Ilharco, A. Aguiar-Ricardo, P. T. Hammond, *Macromolecules* **2011**, *44*, 612.
[17] V. Kozlovskaya, E. Kharlampieva, I. Drachuk, D. Cheng, V. V. Tsukruk, *Soft Matter* **2010**, *6*, 3596.
[18] V. Kozlovskaya, S. Harbaugh, I. Drachuk, O. Shchepelina, N. Kelley-Loughnane, M. Stone, V. V. Tsukruk, *Soft Matter* **2011**, *7*, 2364.

[19] I. Erel, H. Schlaad, A. L. Demirel, *J. Colloid Interface Sci.* **2011**, *361*, 477.
[20] T. G. Shutava, M. D. Prouty, V. E. Agabekov, Y. M. Lvov, *Chem. Lett.* **2006**, *35*, 1144.
[21] D. J. Schmidt, P. T. Hammond, *Chem. Commun.* **2010**, *46*, 7358.
[22] T. Shutava, M. Prouty, D. Kommireddy, Y. Lvov, *Macromolecules* **2005**, *38*, 2850.
[23] I. Erel, Z. Zhu, A. Zhuk, S. A. Sukhishvili, *J. Colloid Interface Sci.* **2011**, *355*, 61.
[24] B.-S. Kim, H.-I. Lee, Y. Min, Z. Poon, P. T. Hammond, *Chem. Commun.* **2009**, *45*, 4194.
[25] J. E. Chung, S. Tan, S. J. Gao, N. Yongvongsoontorn, S. H. Kim, J. H. Lee, H. S. Choi, H. Yano, L. Zhuo, M. Kurisawa, J. Y. Ying, *Nat. Nanotechnol.* **2014**, *9*, 907.
[26] Kh. Kh. Khoultchaev, P. Pang, R. J. Kerekes, P. Englezos, *Can. J. Chem. Eng.* **1998**, *76*, 261.
[27] B. G. Yasnitskii, I. E. Korobeinikova, I. E. Kalashnikova, T. A. Bogun, *Pharm. Chem. J.* **1989**, *23*, 438.
[28] X. Intes, J. Ripoll, Y. Chen, S. Nioka, A. G. Yodh, B. Chance, *Med. Phys.* **2003**, *30*, 1039.
[29] Y. Murakami, M. Yokoyama, H. Nishida, Y. Tomizawa, H. Kurosawa, *Colloids Surf. B Biointerfaces* **2008**, *65*, 186.